Nonbonding Interactions

DOI: 10.1002/ange.200806219

Evidence for C–Cl/C–Br···π Interactions as an Important Contribution to Protein–Ligand Binding Affinity**

Hans Matter, Marc Nazaré, Stefan Güssregen, David W. Will, Herman Schreuder, Armin Bauer, Matthias Urmann, Kurt Ritter, Michael Wagner, and Volkmar Wehner*

The modulation of pharmacokinetic properties by the introduction of halogen atoms into lead structures is a well-established strategy for lead optimization. This includes the blocking of metabolically labile positions of a particular scaffold and the tuning of physicochemical properties to influence membrane permeability and tissue distribution of drug candidates.[1] In particular, the role of organic fluorine atoms, which are often considered as a bioisosteric hydrogen or oxygen replacement,[2] has been extensively investigated on a molecular level, including its effects on protein–ligand interactions in hydrophobic pockets and its involvement as interaction partner.[3] In addition, increasing experimental evidence indicates that organic chlorine and bromine atoms are favorably involved in discrete noncovalent dipolar protein–ligand interactions and thus contribute significantly to binding affinity in molecular recognition.[4] However, much less is known about the nature of nonbonding interactions of organic chlorine and bromine atoms with hydrophobic aromatic protein areas and their contribution to binding affinities.[5]

We recently reported two series of potent inhibitors of the serine protease factor Xa (fXa), an important enzyme in the blood coagulation cascade.[6,7] Analysis of X-ray crystal structures of fXa/inhibitor complexes revealed that the *p*-chlorophenylacetamide and *p*-chlorophenylethyl motifs interact in particular with the aromatic ring of Tyr228 at the back wall of the protease S1 pocket. The remarkable affinity of organic chlorine for aromatic rings has been experimentally observed by us[6,7] and other research groups[5d,8] for fXa and other serine proteases. The deep S1 pocket is very rigid, with a polar Asp189 residue at its base, and often interacts with highly basic, positively charged groups such as amidine in early fXa inhibitors. Thus, an important consequence of the chlorine–Tyr228 interaction is that these motifs, which are detrimental to oral bioavailability, are not required for potent inhibition. This interaction was successfully exploited in our fXa inhibitor program, and led to the identification of the highly potent compound AVE-3247 for clinical development.[9] One favorable characteristic of this compound is the good oral bioavailability associated with replacement of the amidine–Asp189 interaction by the Cl–Tyr228 interaction.

The well-established nature of the interaction led us to study its occurrence in areas other than proteases by 3D searching for close contacts between organic chlorine or bromine atoms and aromatic rings in databases of small-molecule and biomolecular X-ray crystal structures. We also explored its geometry and energetics by experimental and theoretical approaches, namely structure–activity relationships, X-ray crystal structure analysis, and high-level ab initio calculations. Firstly, we systematically investigated the effect of halogens and isosteric replacements on fXa affinity using the recently reported indole-2-carboxamide[6] and 3-oxybenzamide[7] series. The X-ray crystal structure analyses of two inhibitors with factor Xa at resolutions of 2.95 and 2.70 Å (**3a** and **50**,[7] an analogue of **3b**) reveal the organic chlorine atoms in both series to be in close contact with the aromatic ring of Tyr228 (Figure 1a). All derivatives reported in Table 1 were synthesized and tested for fXa inhibition as previously described.[6,7,10]

Compounds **1a** and **1b**, which contain phenyl rings, serve as references for both series. While the addition of a 3-chloro atom lowers affinity, the addition of a 4-chloro atom resulted in very potent inhibitors with an estimated change in free energy of binding ($\Delta\Delta G$) of −10.5 and −8.5 kJ mol^{-1} for **3a** and **3b**, respectively. Replacement of chlorine by bromine at the 4-position also resulted in potent inhibitors, whereas the

Table 1: Structures, factor Xa inhibition constants (K_i), and estimated free energies of binding for inhibitors from two series compared to reference molecules **1a** and **1b**.

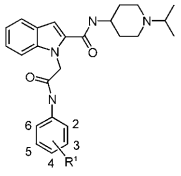

a

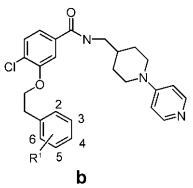

b

Entry	R^1	K_i [nM]	$\Delta\Delta G_{1a\rightarrow Xa}$ [kJ mol^{-1}]	K_i [nM]	$\Delta\Delta G_{1b\rightarrow Xb}$ [kJ mol^{-1}]
1	4-H	204	0	478	0
2	3-Cl	287	+0.84	1931	+3.89
3	4-Cl	3	−10.46	13	−8.51
4	4-F	63	−3.46	102	−3.40
5	4-Br	3	−10.46	36	−5.98
6	4-Me	56	−3.21	124	−2.92
7	4-CN	2855	+6.53	1552	+3.34

[*] Dr. H. Matter, Dr. M. Nazaré, Dr. S. Güssregen, Dr. D. W. Will, Dr. H. Schreuder, Dr. A. Bauer, Dr. M. Urmann, Dr. K. Ritter, Dr. M. Wagner, Dr. V. Wehner
Sanofi-Aventis Deutschland GmbH, Discovery Research
Industriepark Höchst, Building G878
65926 Frankfurt am Main (Germany)
E-mail: hans.matter@sanofi-aventis.com

[**] We thank L. Bayer, A. Sihorsch, and M. Kämmerer for assistance with synthesis, J. Czech for measuring biological affinities, and M. Lorenz and K. H. Baringhaus for useful discussions.

Supporting information for this article is available on the WWW under http://dx.doi.org/10.1002/anie.200806219.

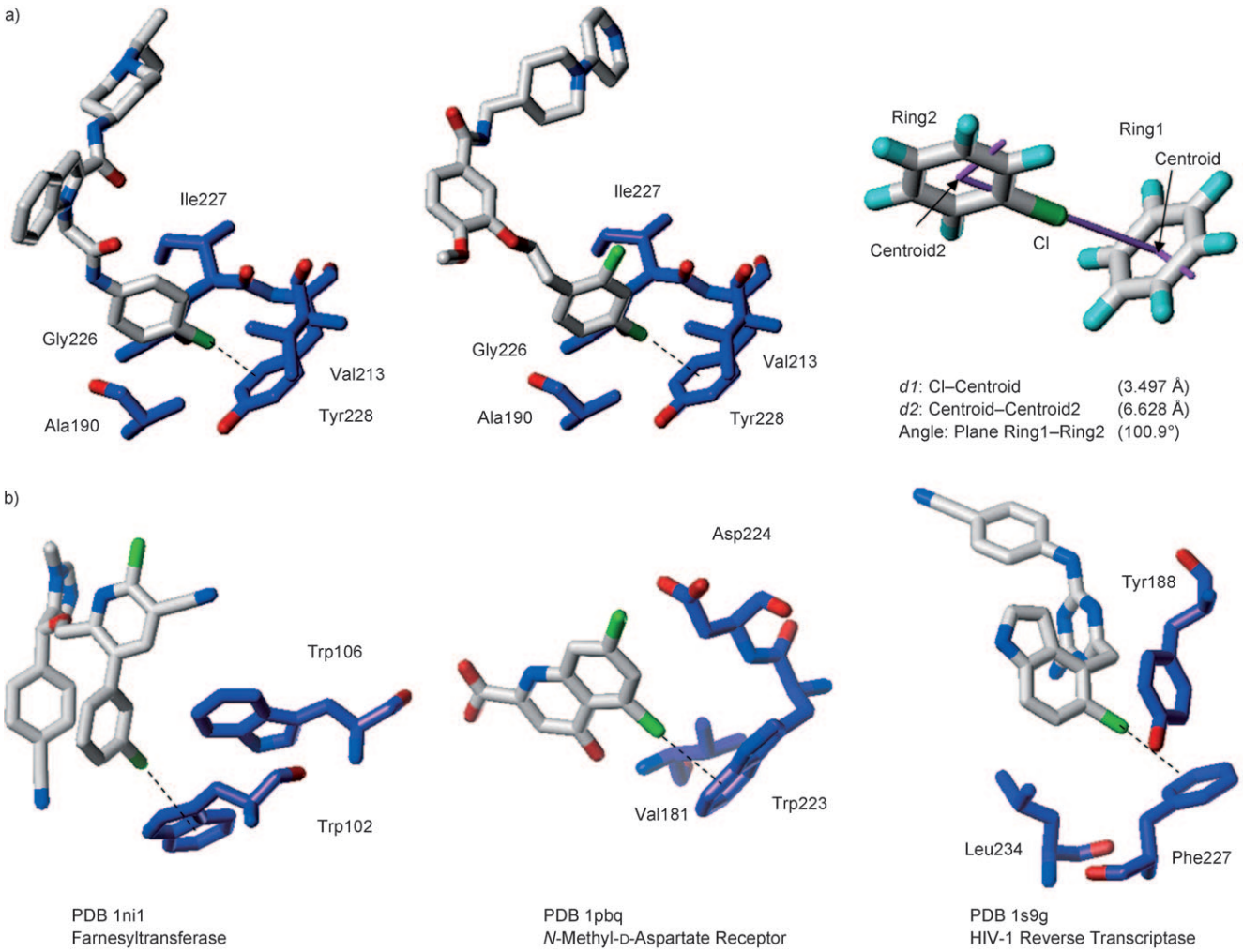

Figure 1. a) Comparison of X-ray crystal structures for indole-2-carboxamide **3a** (left, $K_i = 3$ nM, resolution: 2.95 Å) and 3-oxybenzamide **50**,[7] (center, $K_i = 18$ nM, resolution: 2.7 Å), an analogue of **3b**, complexed with human factor Xa. Only selected residues from the fXa S1 site are shown (purple carbon atoms), C atoms of inhibitors gray, O red, H turquoise, and Cl green; H atoms and structurally conserved water molecules are omitted. Right: Extracted Cl···Tyr228 interaction geometry from the X-ray crystal structure of fXa/**3a** with key distances and angles for database searching and discussion. b) Comparison of X-ray crystal structures for different chlorine-containing ligands complexed with their protein-binding sites, as retrieved from ReliBase+. Left: Farnesyltransferase complexed with imidazole-based inhibitor (PDB 1ni1, 2.3 Å resolution).[17] Center: *N*-methyl-D-aspartate receptor complexed with 5,7-dichlorokynurenic acid (PDB 1pbq, 1.9 Å resolution).[18] Right: HIV-1 reverse transcriptase complexed with R120394 (PDB 1s9g, 2.8 Å resolution).[19]

isosteric 4-methyl substituent has a significantly lower effect, which corresponds to a $\Delta\Delta G$ value of only approximately -3 kJ mol^{-1}. To our surprise, the derivatives with 4-fluoro atoms are not as potent those bearing halogen atoms with larger van der Waals radii (F 1.47, Cl 1.75, Br 1.85, but H 1.20 Å); $\Delta\Delta G$ values of -3.5 kJ mol^{-1} indicate favorable, but weaker interactions. Finally, the polar 4-CN substituent, which is isosteric with bromine, dramatically reduces the binding affinity, which could be attributed to additional repulsive effects within the S1 pocket (van der Waals volumes: F 5.8, Cl 12.0, CH_3 13.7, Br 14.6, CN 14.7 cm^3 mol^{-1} [11]).

The incorporation of 4-chloro and 4-bromo substituents consistently leads to the most potent inhibitors. Several X-ray structures show that these groups are involved in nonbonded interactions with Tyr228. For example, the structures of **3a**,[6] and **50** (the analogue of **3b**)[7,12] reveal the chlorine atom to be invariably located at distances of 3.5–3.7 Å from the centroid of the Tyr228 ring (Figure 1a). The carbon–chlorine bond is oriented toward the plane of the Tyr228 ring; the angles between the ligands and protein aromatic rings are 101° and 106°, respectively. This striking similarity within series and across scaffolds supports our assumption of nearly identical binding geometries for this motif.

Searches in the Cambridge Structural Database (CSD)[13] and RCSB Protein Data Bank[14] provided numerous examples of contacts between organic chlorine or bromine atoms and aromatic rings in small and biomolecular crystal structures. A favorable interaction between chlorine atoms and aromatic amino acids is found 78 times in 52 protein structures in different families, as revealed by ReliBase+ searches[15] with a distance *d1* of 2.8–4.2 Å (Cl···centroid). The hits include 24 serine–protease complexes as well as 28 structures from 14 proteins from other families (see the

Supporting Information). As this nonbonding interaction is not limited to proteases, its significance for protein–ligand recognition is further underscored.

Histograms of both distances *d1* (Cl···centroid) and *d2* (centroid 2···centroid; see the Supporting Information) reveal that the majority of complexes exhibit a Cl–centroid distance *d1* from 3.4 to 3.8 Å, in agreement with fXa X-ray structures (*d1*: 3.49/3.70 Å in Figure 1a). The histogram of the distance *d2* between both ring centroids has a two-maximum distribution. The maximum at 5.2–5.6 Å corresponds to one of the three benzene dimer orientations derived from theoretical calculations,[16] that is, the offset parallel stacking orientation with ring planes parallel to each other (interplanar angle 0°). The second maximum with distances between 6.6–7.0 Å corresponds to variations of the T-shaped edge-to-face and tilted T structures with interplanar angles of about 90°. It includes all protease complexes with the characteristic Cl–Tyr228 interaction plus several examples from other families.

The left panel in Figure 1b shows selected residues from the structure of a farnesyltransferase/inhibitor complex (PDB 1ni1, 2.3 Å).[17] The favorable interaction of the 3-chloro group with the phenyl fragment of Trp102 is indicated. A similar interaction between an organic chlorine atom and Trp223 is present in a complex of the *N*-methyl-D-aspartate (NMDA) receptor with 5,7-dichlorokynurenic acid (PDB 1pbq, 1.9 Å, Figure 1b).[18] For the complex of R120394 with HIV-1 reverse transcriptase (PDB 1s9g, 2.8 Å Figure 1c),[19] a favorable nonbonding interaction is found between the chlorine atom and Phe227.

3D searches for interactions of aromatic rings with fluorine, chlorine, and bromine atoms and methyl groups were carried out with the CSD[13] using the interaction motif in Figure 1a and the following distance boundaries: *d1* from 2.8 to 4.2 Å and *d2* from 5.0 to 8.0 Å. This search resulted in 458 hits with 578 occurrences for intermolecular Cl···ring contacts. The 2D scatter plots in Figure 2 for *d1* (*y* axis; Cl···centroid) versus the interplanar ring angles (Figure 2a, *x* axis) or *d2* (Figure 2c, *x* axis), indicate some geometrical preferences for this interaction. The actual geometry of the fXa/**3a** complex is highlighted in red in both plots. In the scatter plot in Figure 2a, there are two maxima identified at interplanar angles of 1) around 0°, which corresponds to the offset parallel stacking orientation (92 hits, 16%) and 2) from about 60–90°, which relates to edge-to-face orientations (329 hits, 57%). These latter orientations are more frequently populated with an interaction minimum at *d1* ≈ 3.3 Å and multiple small-molecule X-ray structures with similar nonbonded interaction geometries to fXa complexes. Five representative small-molecule structures with interplanar angles of 80 to 90° and distances *d1* from 3.3 to 3.4, all with fXa-like interaction motifs are shown in the Supporting Information.

These CSD derived 2D scatter plots reveal some directional preference of the Cl···centroid interaction with a distribution of approximately edge-to-face-shaped orientations at the second maximum with an interplanar angle between 60 to 90°. The plot for bromine (306 hits, 364 occurrences, see the Supporting Information) reveals a similar preference without strong directionality, while for methyl (1419 hits, 1930 occurrences) and fluorine (142 hits, 190 occurrences) geometries with close contacts to the aromatic rings are widely spread without directional preference. A detailed analysis for electron-rich aromatic rings that interact with chlorine reveals similar frequencies for edge-to-face and offset-parallel-stacking orientations, although the are not statistically significant in all cases (phenol: 19 occurrences, 58%/16%; phenoxy: 44 occurrences, 43%/27%; methylaniline: 81 occurrences, 48%/20% and indole: 6 occurrences: 67%/0%).

Following studies on the benzene dimer[20] and benzene–halomethane complexes,[5c,21] we then calculated MP2 interaction energies of a halobenzene–benzene heterodimer system using four substituents (H, F, Cl, Br) to further investigate this interaction with respect to dimer stabilization energies and directionality.[22] Figure 3a shows a graph of the distance dependency of MP2 heterodimer interaction energies (kJ mol^{-1}). The distance between points B (that is, centroid ring 1) and A (centroid 2, ring 2) was systematically varied in 0.25 Å steps along the path from A to B for H, F, Cl, and Br atoms attached to the first aromatic ring that approaches the plane of the second ring in the heterodimer. For chlorine, the minimum MP2 interaction energy of −7.09 kJ mol^{-1} is found at a distance *d2* of 6.75 Å, which is in agreement with X-ray crystal structures and statistical preferences from CSD and RCSB. Energy

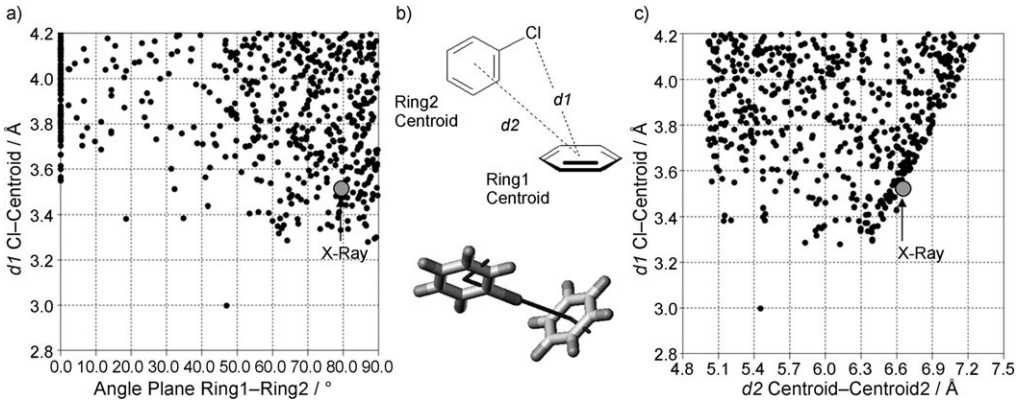

Figure 2. Scatter plots of *d1* (distance Cl···centroid) on the *y* axis versus interplanar angle between both aromatic rings on the *x* axis (a) or *d2* (distance centroid 2···centroid) on the *x* axis (c) for CSD search based on the chlorine substituent and 458 hits with 578 occurrences. The interaction geometry from the fXa/**3a** complex is highlighted by a gray circle. One outlier (ZIVKIV), with a very close Cl···centroid distance of 3.0 Å and an interplanar angle of about 50° is caused by out-of-plane distortion of the C–Cl bond because of nonbonding contact to a neighboring aromatic ring. The interaction geometry used for searching is shown in (b).

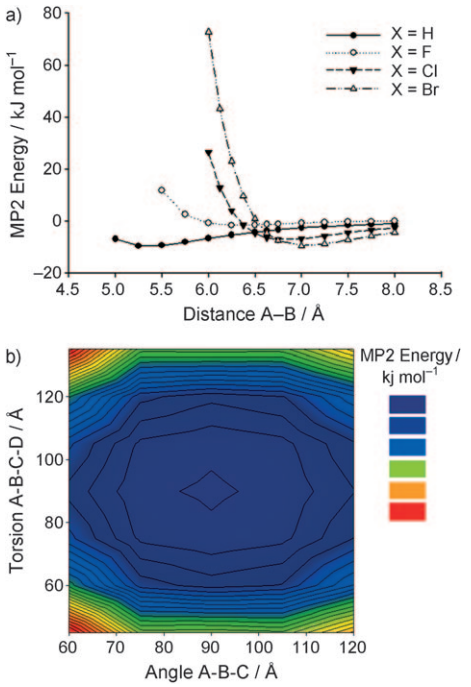

Figure 3. a) Plot of MP2 interaction energies [kJ mol^{-1}] versus nonbonding interaction distance A–B [Å] for ab initio calculations of four different heterodimers with H (black circles), F (open circles), Cl (black triangles), and Br (open triangles) as aromatic substituents approaching the second aromatic ring. b) Potential energy surfaces from MP2 interaction energies for different heterodimer configurations at constant Cl···centroid distances. The color code on the right indicates the MP2 energy distribution [kJ mol^{-1}].

values computed at geometries with $d2 < 6.7$ Å are much higher because of repulsion, while for larger distances this energy value approaches zero. At a distance of 7.5 Å, remarkable dimer energies of -5 kJ mol^{-1} are still observed, in agreement with the broad scattering of CSD results (Figure 2). This heterodimer interaction minimum is shifted towards 7.0 Å for bromine because of its larger van der Waals radius, with a significant minimum MP2 interaction energy value of -9.49 kJ mol^{-1}. This result indicates a more favorable interaction for bromine than chlorine with the aromatic plane of its nonbonded partner, which is in agreement with the experimental data (Table 1). In contrast, the interaction maximum for fluorine is shifted to 6.25 Å, but with a much weaker aromatic plane interaction, as indicated by a heterodimer MP2 interaction energy value of -1.62 kJ mol^{-1}. This minimum again agrees with the smaller van der Waals radius of the halogen atom. The very low polarizability, high electronegativity, and three tightly bound nonbonding electron pairs of fluorine result in stronger repulsive and electrostatic interactions. These results are consistent with other ab initio calculations at a comparable level for the fluorobenzene···
benzene complex, in which the orientation with the fluorine atom pointing towards the plane of the benzene ring was not found to be energetically very favorable.[23] Finally, the geometries for the approach of a hydrogen atom to the second aromatic ring are in very good agreement with other accounts of aromatic–aromatic "edge-to-face" interactions[24,25,26,16] with a minimum at 5.25 Å and a dimer MP2 interaction energy value of -9.54 kJ mol^{-1}. When the benzene ring is replaced by phenol as an electron-rich aromatic system, the MP2 interaction energies are lowered for chlorine (-14.95 kJ mol^{-1}) at the X-ray-determined distance of 6.68 Å between two centroids. Bromine shows the same trend although a stronger interaction is present (-23.53 kJ mol^{-1}), while the interactions of fluorine and hydrogen are significantly weaker than that of bromine (-6.66 and -7.41 kJ mol^{-1}), but stronger than those of benzene (-1.84 and -3.73 kJ mol^{-1}) at similar distances. A similar stabilization effect is expected for the electron-rich indole system of tryptophan.

These heterodimer MP2 interaction energies and geometries agree with the estimated free energy of binding for scaffolds with 4-Cl substituents (Table 1), although ab initio calculations only account for the enthalpic part of nonbonding interactions. $\Delta\Delta G$ values of -10.46 and -8.51 kJ mol^{-1} were estimated from binding affinities for **3a** and **3b**, respectively. In addition, the experimental distances *d2* are in agreement with 6.63 Å for the X-ray geometry. Furthermore, the agreement between the MP2 interaction energies and $\Delta\Delta G$ values of chlorine and bromine, and the less favorable energy contribution of fluorine are remarkable, with a $\Delta\Delta G$ value of around -3.5 kJ mol^{-1} and an MP2 energy of -1.6 kJ mol^{-1}. Only the MP2 interaction energy of -9.5 kJ mol^{-1} for hydrogen as "substituent" is not in agreement with the estimated free energy of binding, which is due to steric constraints imposed by the S1 pocket preventing the inhibitor aromatic ring from approaching Tyr228 for a favorable CH···π contact at shorter distances.[27] The shapes of the potentials are comparable with the results from simpler systems,[20,21] which are flat near the minima. Substantial attraction still exists, even if the molecules are well separated, which suggests that the major source of attraction in these complexes is not short-range interactions ($E \approx e^{-\alpha R}$), such as backbonding effects of π electrons on unoccupied *d* orbitals, but long-range interactions ($E \approx R^{-n}$) such as electrostatic and dispersion interactions.

The angular dependency of the interaction for chlorine atoms (Figure 3b) demonstrates that the intermolecular interaction potential surface from ab initio calculations at the MP2/aug-cc-pVDZ level is extremely flat, without strong directional preferences. A broad minimum between 65° and 115° of the angle A-B-C is in agreement with the results of the CSD searches. This demonstrates that dispersion, that is, London forces and not electrostatic interactions, are the major source of attraction, as the latter would be highly orientation-dependent. However it is likely that different interaction modes make weak contributions to various extents at different separations, such as electrostatic interactions at shorter distances.

In summary, we have presented the first systematic study of the Cl/Br···π interaction as key factor for the identification of the potent and orally bioavailable molecule AVE-3247, which entered clinical development. Our investigation of this interaction is based on binding affinities, X-ray crystal structures, 3D database searches, and ab initio calculations.

All methods are remarkably consistent in terms of preferred geometries and directional preferences for this interaction, which lead to a stabilization of complex structures of up to $-10\ kJ\,mol^{-1}$. These interactions have a characteristic geometry: the chlorine atom tends to reside on top of the plane of the neighboring aromatic ring with the Cl–C bond approaching its aromatic plane from an angle of 60–90°. Remarkably, this motif stabilizes small-molecule crystal structures and protein–ligand complexes from multiple families, which indicates that this interaction is of a more general nature and not defined solely by the nature of the pocket, or the protein in which the interaction takes place. We conclude that this Cl/Br···π interaction might be of general use in structure-based design towards optimized "edge-to-face" interactions for aromatic amino acids. A detailed understanding of the implications for this general nonbonded interaction motif in protein–ligand complexes can emerge from these studies.

Received: December 19, 2008
Published online: March 17, 2009

Keywords: ab initio calculations · halogens · inhibitors · noncovalent interactions · π interactions

[1] a) H.-J. Böhm, D. Banner, S. Bendels, M. Kansy, B. Kuhn, K. Mueller, U. Obst-Sander, M. Stahl, *ChemBioChem* **2004**, *5*, 637 – 643; b) G. Gerebtzoff, X. Li-Blatter, H. Fischer, A. Frentzel, A. Selig, *ChemBioChem* **2004**, *5*, 676 – 684; c) W. K. Hagmann, *J. Med. Chem.* **2008**, *51*, 4359 – 4369; d) K. Park, N. R. Kitteringham, P. M. O'Neill, *Annu. Rev. Pharmacol. Toxicol.* **2001**, *41*, 443 – 470.

[2] a) E. Schweizer, A. Hoffmann-Röder, K. Scharer, J. A. Olsen, C. Fah, P. Seiler, U. Obst-Sander, B. Wagner, M. Kansy, F. Diederich, *ChemMedChem* **2006**, *1*, 611 – 621; b) P. Shah, A. D. Westwell, *J. Enzyme Inhib. Med. Chem.* **2007**, *22*, 527 – 540; c) F. Leroux, *ChemBioChem* **2004**, *5*, 644 – 649.

[3] a) J. D. Dunitz, R. Taylor, *Chem. Eur. J.* **1997**, *3*, 89 – 98; b) J. A. Olsen, D. W. Banner, P. Seiler, B. Wagner, T. Tschopp, U. Obst-Sander, M. Kansy, K. Müller, F. Diederich, *ChemBioChem* **2004**, *5*, 666 – 675; c) J. A. Olsen, D. W. Banner, P. Seiler, U. Obst-Sander, A. D'Arcy, M. Stihle, K. Müller, F. Diederich, *Angew. Chem.* **2003**, *115*, 2611 – 2615; *Angew. Chem. Int. Ed.* **2003**, *42*, 2507 – 2511; d) E. Carosati, S. Sciabola, G. Cruciani, *J. Med. Chem.* **2004**, *47*, 5114 – 5125.

[4] a) P. Metrangolo, F. Meyer, T. Pilati, G. Resnati, G. Terraneo, *Angew. Chem.* **2008**, *120*, 6206 – 6220; *Angew. Chem. Int. Ed.* **2008**, *47*, 6114 – 6127; b) P. Auffinger, F. A. Hays, E. Westhof, P. S. Ho, *Proc. Natl. Acad. Sci. USA* **2004**, *101*, 16789 – 16794; c) A. R. Voth, P. S. Ho, *Curr. Top. Med. Chem.* **2007**, *7*, 1336 – 1348.

[5] a) I. Saraogi, V. G. Vijay, S. Das, K. Sekar, T. N. Row, *Cryst. Eng.* **2003**, *6*, 69 – 77; b) D. Swierczynski, R. Luboradzki, G. Dolgonos, J. Lipkowski, H.-J. Schneider, *Eur. J. Org. Chem.* **2005**, 1172 – 1177; c) Y. N. Imai, Y. Inoue, I. Nakanishi, K. Kitaura, *Protein Sci.* **2008**, *17*, 1129 – 1137; d) Y. Shi, D. Sitkoff, J. Zhang, H. E. Klei, K. Kish, E. C.-K. Liu, K. S. Hartl, S. M. Seiler, M. Chang, C. Huang, S. Youssef, T. E. Steinbacher, W. A. Schumacher, N. Grazier, A. Pudzianowski, A. Apedo, L. Discenza, J. Yanchunas, P. D. Stein, K. S. Atwal, *J. Med.Chem.* **2008**, *51*, 7541 – 7551.

[6] M. Nazaré, D. W. Will, H. Matter, H. Schreuder, K. Ritter, M. Urmann, M. Essrich, A. Bauer, M. Wagner, J. Czech, M. Lorenz, V. Laux, V. Wehner, *J. Med. Chem.* **2005**, *48*, 4511 – 4525.

[7] H. Matter, D. W. Will, M. Nazaré, H. Schreuder, V. Laux, V. Wehner, *J. Med. Chem.* **2005**, *48*, 3290 – 3312.

[8] a) T. J. Tucker, S. F. Brady, W. C. Lumma, S. D. Lewis, S. J. Gardell, A. M. Naylor-Olsen, Y. Yan, J. T. Sisko, K. J. Stauffer, B. J. Lucas, J. J. Lynch, J. J. Cook, M. T. Stranieri, M. A. Holahan, E. A. Lyle, E. P. Baskin, I. W. Chen, K. B. Dancheck, J. A. Krueger, C. M. Cooper, J. P. Vacca, *J. Med. Chem.* **1998**, *41*, 3210 – 3219; b) M. Adler, M. J. Kochanny, B. Ye, G. Rumennik, D. R. Light, S. Biancalana, M. Whitlow, *Biochemistry* **2002**, *41*, 15514 – 15523; c) M. T. Stubbs, S. Reyda, F. Dullweber, M. Moller, G. Klebe, D. Dorsch, W. W. K. R. Mederski, H. Wurziger, *ChemBioChem* **2002**, *3*, 246 – 249; d) S. Maignan, J.-P. Guilloteau, Y. M. Choi-Sledeski, M. R. Becker, W. R. Ewing, H. W. Pauls, A. P. Spada, V. Mikol, *J. Med. Chem.* **2003**, *46*, 685 – 690; e) S. Roehrig, A. Straub, J. Pohlmann, T. Lampe, J. Pernerstorfer, K.-H. Schlemmer, P. Reinemer, E. Perzborn, *J. Med. Chem.* **2005**, *48*, 5900 – 5908; f) M. J. Hartshorn, C. W. Murray, A. Cleasby, M. Frederickson, I. J. Tickle, H. Jhoti, *J. Med. Chem.* **2005**, *48*, 403 – 413.

[9] M. Nazare, M. Essrich, D. W. Will, H. Matter, K. Ritter, Kurt, V. Wehner, PCT Int. Appl. EP 1314733, **2003**.

[10] M. Nazaré, H. Matter, O. Klingler, F. Al-Obeidi, H. Schreuder, G. Zoller, J. Czech, M. Lorenz, A. Dudda, A. Peyman, H. P. Nestler, M. Urmann, A. Bauer, V. Laux, V. Wehner, D. W. Will, *Bioorg. Med. Chem. Lett.* **2004**, *14*, 2801 – 2805.

[11] A. Bondi, *J. Phys. Chem.* **1964**, *68*, 441 – 451.

[12] Please note the additional *ortho*-chlorine atom in Figure 1b (center) for the analogue of compound **3b**. Comparative studies show that this additional substituent does not affect the overall binding mode in S1.[6,10]

[13] CSD version 5.26 of November 2004, which holds over 325000 small-molecule crystal structures, obtained from The Cambridge Crystallographic Data Centre (CCDC), 12 Union Road, Cambridge, CB2 1EZ, UK (http://www.ccdc.cam.ac.uk). The search using ConQuest 1.7 (CCDC) was limited to neutral organic compounds excluding experimental disorder and metal–organic and polymeric compounds.

[14] a) RCSB Protein Data Bank (http://www.rcsb.org/pdb); b) H. M. Berman, J. Westbrook, Z. Feng, G. Gilliland, T. N. Bhat, H. Weissig, I. N. Shindyalov, P. E. Bourne, *Nucleic Acids Res.* **2000**, *28*, 235 – 242.

[15] a) Searching the RCSB with over 32,000 entries was done by using ReliBase+ version 1.3.1 (May 2005) from Cambridge Crystallographic Data Centre (CCDC), 12 Union Road, Cambridge CB2 1EZ, UK. Only X-ray structures with a resolution < 3.5 Å were searched; b) M. Hendlich, A. Bergner, J. Günther, G. Klebe, *J. Mol. Biol.* **2003**, *326*, 607 – 620.

[16] a) P. Hobza, H. L. Selzle, E. W. Schlag, *Chem. Rev.* **1994**, *94*, 1767 – 1785; b) W. B. Jennings, B. M. Farrell, J. F. Malone, *Acc. Chem. Res.* **2001**, *34*, 885 – 894.

[17] Y. Tong, N. H. Lin, L. Wang, L. Hasvold, W. Wang, N. Leonard, T. Li, Q. Li, J. Cohen, W. Z. Gu, H. Zhang, V. Stoll, J. Bauch, K. Marsh, S. H. Rosenberg, H. L. Sham, *Bioorg. Med. Chem. Lett.* **2003**, *13*, 1571 – 1574.

[18] H. Furukawa, E. Gouaux, *EMBO J.* **2003**, *22*, 2873 – 2885.

[19] M. Vinkers, F. Daeyaert, D. W. Ludovici, M. J. Kukla, B. De Corte, R. W. Kavash, C. Y. Ho, H. Ye, M. A. Lichtenstein, K. Andries, R. Pauwels, M.-P. de Béthune, P. L. Boyer, P. Clark, S. H. Hughes, P. A. J. Janssen, E. Arnold, *J. Med. Chem.* **2004**, *47*, 2550 – 2560.

[20] For a comprehensive overview on theoretical studies for the benzene dimer, see a) M. O. Sinnokrot, E. F. Valeev, C. D. Sherril, *J. Am. Chem. Soc.* **2002**, *124*, 10887 – 10893; b) S. Tsuzuki, K. Honda, T. Uchimaru, M. Mikami, K. Tanabe, *J. Am. Chem. Soc.* **2002**, *124*, 104 – 112; c) P. Hobza, H. L. Selzle, E. W. Schlag, *J. Phys. Chem.* **1996**, *100*, 18790 – 18794, and references therein.

[21] S. Tsuzuki, K. Honda, T. Uchimaru, M. Mikami, K. Tanabe, *J. Phys. Chem. A* **2002**, *106*, 4423 – 4428.
[22] MP2 interaction energies were calculated by using Dunning's correlation consistent basis set aug-cc-pVDZ (R. A. Kendall, T. H. Dunning, R. Harrison, *J. Chem. Phys.* **1992**, *96*, 6796 – 6806). Starting geometries were obtained by superimposing the monomers, geometrically optimized at the same level of theory, onto corresponding atoms from the fXa/**3a** X-ray crystal structure. The monomers were kept frozen in all heterodimer calculations, and the basis set superposition error (BSSE; B. J. Ransil, *J. Chem. Phys.* **1961**, *34*, 2109 – 2118) was corrected for all calculations by using the counterpoise method (S. F. Boys, F. Bernardi, *Mol. Phys.* **1970**, *19*, 553 – 566). The NWCHEM 4.6 program (T. P. Straatsma, E. Apra, T. L. Windus, E. J. Bylaska, W. de Jong, S. Hirata, M. Valiev, M. T. Hackler, L. Pollack, R. J. Harrison, M. Dupuis, D. M. A. Smith, J. Nieplocha, V. Tipparaju, M. Krishnan, A. A. Auer, E. Brown, G. Cisneros, G. I. Fann, H. Fruchtl, J. Garza, K. Hirao, R. Kendall, J. A. Nichols, K. Tsemekhman, K. Wolinski, J. Anchell, D. Bernholdt, P. Borowski, T. Clark, D. Clerc, H. Dachsel, M. Deegan, K. Dyall, D. Elwood, E. Glendening, M. Gutowski, A. Hess, J. Jaffe, B. Johnson, J. Ju, R. Kobayashi, R. Kutteh, Z. Lin, R. Littlefield, X. Long, B. Meng, T. Nakajima, S. Niu, M. Rosing, G. Sandrone, M. Stave, H. Taylor, G. Thomas, J. van Lenthe, A. Wong, and Z. Zhang, NWChem, A Computational Chemistry Package for Parallel Computers, Version 4.6, 2004, Pacific Northwest National Laboratory, Richland, Washington 99352-0999, USA) was used for all calculations.
[23] A. DerHovanessian, J. B. Doyon, A. Jain, P. R. Rablen, A.-M. Sapse, *Org. Lett.* **1999**, *1*, 1359 – 1362.
[24] L. J. Andrews, *Chem. Rev.* **1954**, *54*, 713 – 776.
[25] a) S. K. Burley, G. A. Petsko, *Science* **1985**, *229*, 23 – 28; b) S. K. Burley, G. A. Petsko, *J. Am. Chem. Soc.* **1986**, *108*, 7995 – 8001.
[26] E. A. Meyer, R. K. Castellano, F. Diederich, *Angew. Chem.* **2003**, *115*, 1244 – 1287; *Angew. Chem. Int. Ed.* **2003**, *42*, 1210 – 1250.
[27] Docking and minimization of inhibitors within the fXa binding site were carried out by using the program QXP (C. McMartin, R. S. Bohacek, *J. Comput. Aided Mol. Des.* **1997**, *11*, 333 – 344) employing a modified AMBER force field (S. J. Weiner, P. A. Kollman, D. A. Case, U. C. Singh, C. Ghio, G. Algona, S. Profeta, P. Weiner, *J. Am. Chem. Soc.* **1984**, *106*, 765 – 784) and the X-ray structures of **3a** and **50**, respectively.

